Supporting Information

Berné and Tielens 10.1073/pnas.1114207108

SI Text

1 Physical Conditions in NGC 7023. ***1.1 General properties.*** NGC 7023 is a widely studied photodisociation region. We briefly review the information on physical conditions available in the literature. The nebula has an hourglass-shaped, low-density cavity, which was opened in the dense molecular cloud by the winds of the young Be star (1). The formation of C_{60} is seen to occur inside this cavity (See Fig. 1 in the main text) in regions particularly close to the star (10″ to 40″). In the next sections we discuss the values we adopt for radiation field and gas density in the cavity.

1.2 Radiation field. The intensity of the radiation field in the cavity, G_0, can be derived based on the spectral type and flux of the star diluted by the square of the distance from the star. Doing this exercise, Joblin et al. (2) find that the radiation field is $G_0 = 2{,}600$ at a distance of 40″ from the star [similar to the value found by Rogers et al. (3) and Chokshi et al. (4). Using this value and spherical dilution, we derive the range of radiation fields covered in the cut where we study C_{60} and polycyclic aromatic hydrocarbon (PAH) evolution (Figs. 1 and 2). We find $G_0 = 3.0 \times 10^4$ at the peak of C_{60} abundance (12″ from the star) and $G_0 = 3.4 \times 10^3$ at the minimum of C_{60} abundance (35″ from the star). Fuente et al. (5) have reported the highest value of radiation field in the photodissociation region (PDR) with $G_0 = 1 \times 10^4$ at the position of the H_2 filaments at 46″ from the star. This would correspond to values of $G_0 = 1.7 \times 10^4$ and $G_0 = 1.5 \times 10^5$ at the edges of the cut (respectively, 35″ and 12″ from the star). We therefore adopt average values $G_0 = 1.0 \pm 0.7 \times 10^4$ and $G_0 = 1.0 \pm 0.7 \times 10^5$ at 35 and 12″ from the star.

1.3 Density in the cavity. The density of the atomic gas in this region is difficult to derive directly, but can be constrained from observations of the surrounding molecular cloud. More specifically, the density derived from CO lines by Gerin et al. (6) in the back wall of the cavity point to a value of $n_H^{\rm Mol} \sim 3{,}000$ cm^{-3}. The atomic gas well within the cavity, is expected to be at least an order of magnitude hotter, and hence an order of magnitude less dense if we consider pressure equilibrium (i.e., $n_H^{\rm Cav} \sim 300$). Rogers et al. (3) find that $n_H^{\rm Mol}/n_H^{\rm Cav} = 10^{-35}$, which then implies $n_H^{\rm Cav} = 85$–300. Joblin et al. (2) quote a value of 100 cm^{-3} for $n_H^{\rm Cav}$. A more direct estimation of the column density of warm atomic gas can be derived from the dust emission. Because we have seen that dust temperature increases when getting closer to the star (see first section of this document), this implies that this emission indeed comes form the cavity and not from the wall behind. Using the DUSTEM (7) model, we can reproduce the observed emission in the Photodetector Array Camera end Spectrometer 70-μm filter at a distance of 35″ from the star (approximately 1 Jy/pixel or 2,300 MJy.sr^{-1}), for a radiation field of $G_0 = 10^4$, and leaving the column density as a free parameter. This yields $N_H = 2 \times 10^{19}$ cm^{-2} for the cavity, which with a physical size of 5.7×10^{17} cm ($2 \times 35''$ at 400 pc) corresponds to $n_H^{\rm Cav} = 45$ cm^{-2}, somewhat lower than other estimates based on PDR or molecular tracers. Note that this determination does not depend significantly on the accuracy of determination of radiation field in the considered range of G_0 (see ref. 7, figure 7). We keep $n_H^{\rm Cav} = 50$ as lower limit and $n_H^{\rm Cav} = 250$ as upper limit and adopt $n_H^{\rm Cav} = 150 \pm 100$ cm^{-3}.

1.4 G_0/n_H. Using the adopted average density and radiation field values we can obtain G_0/n_H needed to estimate the dehydrogenation efficiency (see *Graphene Formation* in the main text). We find $G_0/n_H = 65 \pm 45$ at 35″ from the star and $G_0/n_H = 650 \pm 450$ at 12″ from the star. From these numbers, we define the "broad" and "narrow" domains of values of G_0/n_H expected in the cut in NGC 7023, [20–1100] and [105–200], respectively. These are represented graphically in Fig. 4 over the dehydrogenation stability curve.

1. Fuente A, Martin-Pintado J, Bachiller R, Neri R, Palla F (1998) Progressive dispersal of the dense gas in the environment of early type and late-type Herbig Ae-Be stars. *Astron Astrophys* 334:253–263.
2. Joblin C, et al. (2010) Gas morphology and energetics at the surface of PDRs: New insights with Herschel observations of NGC 7023. *Astron Astrophys* 521:25–29.
3. Rogers C, Heyer MH, Dewdney PE (1995) H I, CO, and IRAS observations of NGC 7023 *Astrophys J* 442:694–713.
4. Chokshi A, Tielens AGGM, Werner MW, Castelaz MW (1988) C II 158 micron and O I 63 micron observations of NGC 7023—A model for its photodissociation region *Astrophys J* 334:803–814.
5. Fuente A, et al. (1999) Infrared Space Observatory observations toward the Reflection Nebula NGC 7023: A nonequilibrium ortho-to-para-H_2 ratio. *Astrophys J* 518:45.
6. Gerin M, Phillips TG, Keene J, Betz AL, Boreiko RT (1998) CO, C I, and C II observations of NGC 7023 *Astrophys J* 500:329.
7. Compiègne M, et al. (2011) The global dust SED: tracing the nature and evolution of dust with DustEM. *Astron Astrophys* 525:103.

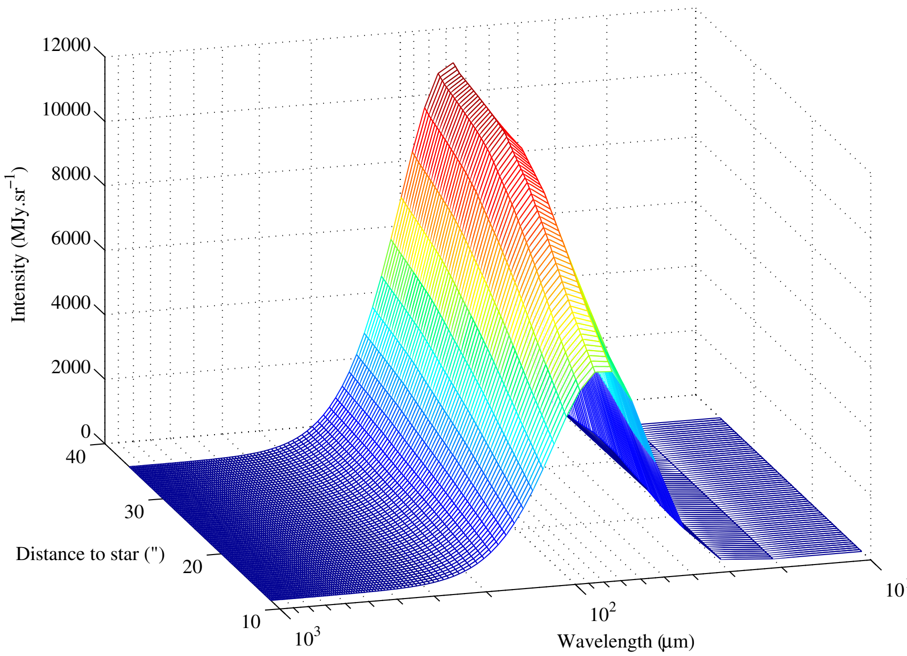

Fig. S1. Fitted modified black bodies to the SEDs observed with Herschel in the cross-cut from position (1) to (2) shown in Fig. 1.

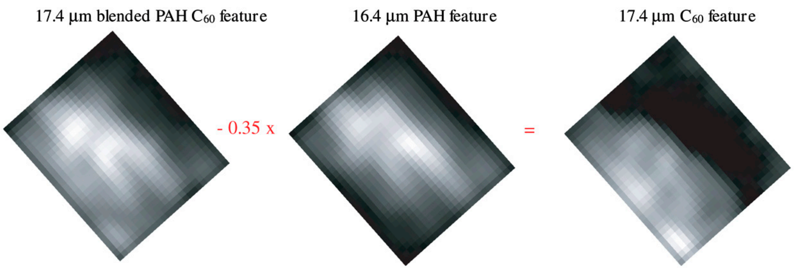

Fig. S2. Subtraction of the contamination of PAHs in the 17.4-µm band.

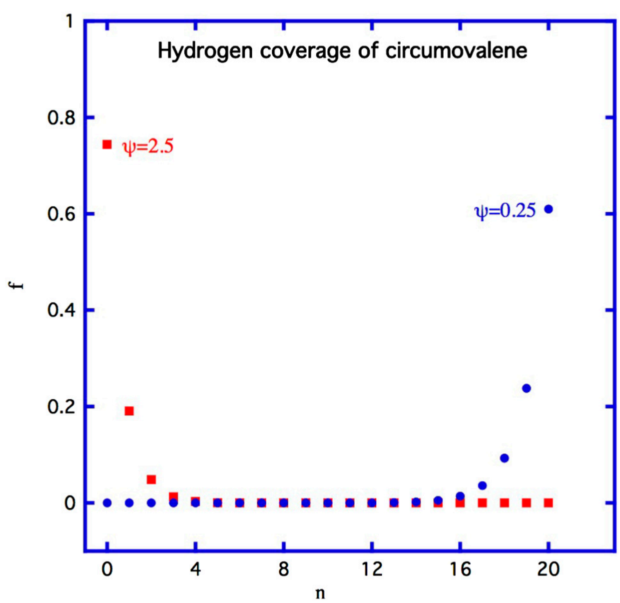

Fig. S3. The relative abundance of circumovalene and its partial dehydrogenated derivatives, $C_{66}H_n$, for two values of the dissociation parameter, ψ.

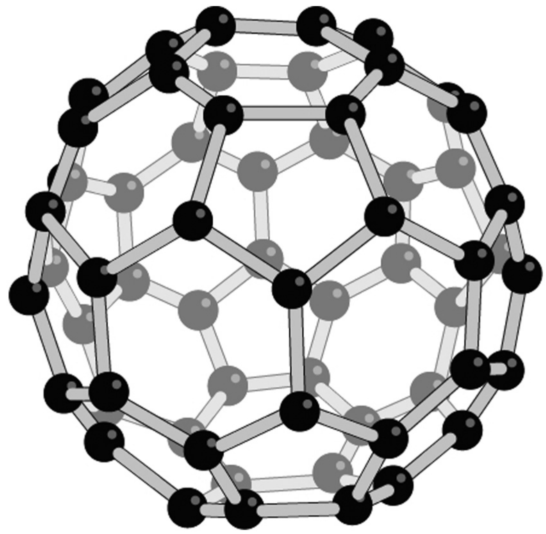

Movie S1. Conversion of graphene into C_{60}. This video shows schematically how graphene can be converted into C_{60}. We start with a sheet of graphene where carbon atoms are arranged in a hexagonal network. Under UV irradiation, C atoms are lost in the hexagons situated at the edge of the graphene flake and converted into pentagons (shown in orange). The formation of pentagons stresses the molecule forcing it to curve. When several pentagons have been formed, they can migrate inside the molecule. Finally, when 12 pentagons have been formed and when each carbon atom belongs to both a pentagon and a hexagon, the molecule closes into C_{60}.

Movie S1 (MOV)